JACS
JOURNAL OF THE AMERICAN CHEMICAL SOCIETY
Communication
pubs.acs.org/JACS

Designed Diblock Oligonucleotide for the Synthesis of Spatially Isolated and Highly Hybridizable Functionalization of DNA–Gold Nanoparticle Nanoconjugates

Hao Pei,[†,§] Fan Li,[†,§] Ying Wan,[‡] Min Wei,[†] Huajie Liu,*[,†] Yan Su,[‡] Nan Chen,[†] Qing Huang,[†] and Chunhai Fan*[,†]

[†]Laboratory of Physical Biology, Shanghai Institute of Applied Physics, Chinese Academy of Sciences, Shanghai 201800, China
[‡]School of Mechanical Engineering, Nanjing University of Science and Technology, Nanjing 210094, China

Supporting Information

ABSTRACT: Conjugates of DNA and gold nanoparticles (AuNPs) typically exploit the strong Au–S chemistry to self-assemble thiolated oligonucleotides at AuNPs. However, it remains challenging to precisely control the orientation and conformation of surface-tethered oligonucleotides and finely tune the hybridization ability. We herein report a novel strategy for spatially controlled functionalization of AuNPs with designed diblock oligonucleotides that are free of modifications. We have demonstrated that poly adenine (polyA) can serve as an effective anchoring block for preferential binding with the AuNP surface, and the appended recognition block adopts an upright conformation that favors DNA hybridization. The lateral spacing and surface density of DNA on AuNPs can also be systematically modulated by adjusting the length of the polyA block. Significantly, this diblock oligonucleotide strategy results in DNA–AuNPs nanoconjugates with high and tunable hybridization ability, which form the basis of a rapid plasmonic DNA sensor.

Nucleic acids have been increasingly exploited for material purposes.[1] Particularly, the unparallel self-assembly ability of DNA has proven of high utility in constructing elaborate nanostructures[2] and nanomachines[3] and organizing natural or synthetic nanomaterials in a precise manner.[4] One of the key challenges toward such applications lies in reliable preparation of conjugates of DNA and inorganic nanomaterials (e.g., gold nanoparticles, AuNPs), which often requires chemical modification of oligoncleotides.[5] DNA–AuNPs conjugates are one of the most versatile hybrid bionanomaterials for various applications.[6] Such nanoconjugates typically exploit the well-established strong Au–S chemistry to self-assemble thiolated oligonucleotides at the surface of AuNPs.[7] While this widely employed strategy has proven highly useful in many applications, it remains challenging to precisely control the orientation and conformation of surface-tethered oligonucleotides and finely tune the hybridization ability.[8] Here we propose a new strategy for spatially controlled functionalization of AuNPs with designed, modification-free, diblock DNA oligonucleotides and demonstrate rapid hybridization in colorimetric DNA detection with plasmonic nanoconjugates.

Nanomaterials with heterofunctional domains often possess attractive features.[9] Block copolymers with two or more distinct functional segments offer one possible route to assembly of higher-order, complex nanostructures with various applications.[10] The combination of distinctive "blocks" has appealing features of integrating multiple functions and promoting stability and performance. Since DNA is a natural polymer with excellent recognition ability as well as structural and functional diversity (e.g., aptamers, DNAzyme),[11] it may serve as a versatile building block either when coupled with synthetic polymers[12] or by itself.[13] Particularly, given the commercial power in mass-producing oligonucleotides of almost any given sequence, copolymers with pure DNA sequences can be readily available with high purity and low cost, offering unprecedented convenience in design flexibility and reliability in quality control. For the purpose of bioconjugation with AuNPs, it is a necessity to have a copolymer having an anchoring segment for binding with AuNPs and a function segment for recognition. Previous studies with planar Au substrates have shown that poly adenine (polyA) sequences containing multiple consecutive adenines preferentially adsorb Au with high affinity, even comparable to Au–S chemistry.[14] We then explore the possibility of using polyA as the anchoring block (shown in Scheme S1, Supporting Information, SI) on the nanoscale, highly curved surface of AuNPs (13 nm in diameter).

To substantiate that polyA can replace the thiol group by strongly binding to AuNPs and competitively displacing other base combinations, we prepared thiol-free diblock oligonucleotides containing the $polyA_{10}$ block and the recognition block (Scheme S1, SI). They were incubated with AuNPs with a protocol similar to that of thiol-DNA.[7] A thiolated oligonucleotide without the polyA block and another oligonucleotide containing the non-polyA block were employed as controls. While we obtained red-colored solutions in all situations, suggesting the formation of well-dispersed nanoconjugates,[7] they showed remarkably different stability toward salt-inducing aggregation. Oligonucleotides with either the polyA block or thiol resulted in highly stable nanoconjugates that remained to be red even in a solution containing 0.3 M NaCl (Figure S1, SI), while AuNPs conjugated with the one with the non-polyA block slightly changed the color even at 20 mM NaCl and then

Received: April 29, 2012
Published: July 16, 2012

dx.doi.org/10.1021/ja304118z | J. Am. Chem. Soc. 2012, 134, 11876–11879

to blue colors at higher ionic strengths, an effect due to plasmonic shift in response to nanoparticle aggregation (Figure S1, SI).

We further assess the stability of AuNPs with diblock oligonucleotides. By using fluorophore-labeled diblock oligonucleotides, we monitored the temperature-dependent desorption from AuNPs. AuNPs capped with the diblock oligonucleotide were highly resistant to heating, and only few strands broke off from the surface even at a high temperature of 90 °C, exhibiting comparable stability to thiol-DNA (Figure S2, SI). Since thymine is the complementary base of adenine, we also tested the resistance of a series of diblock DNA–AuNPs conjugates ($polyA_{10}$, $polyA_{15}$, $polyA_{20}$, $polyA_{30}$) to the presence of polyT strands ($polyT_{10}$, $polyT_{15}$, $polyT_{20}$, $polyT_{30}$). We observed that only few polyA on AuNPs were displaced through possible A-T base pairing (Figure S3), suggesting that the strong absorption of polyA blocks at the AuNPs surface.

Given the high-adsorption affinity of polyA on AuNPs, we were inspired to vary the length of polyA blocks to spatially control the assembly of oligonucleotides on AuNPs (Figure 1a). We quantified the surface density of assembled

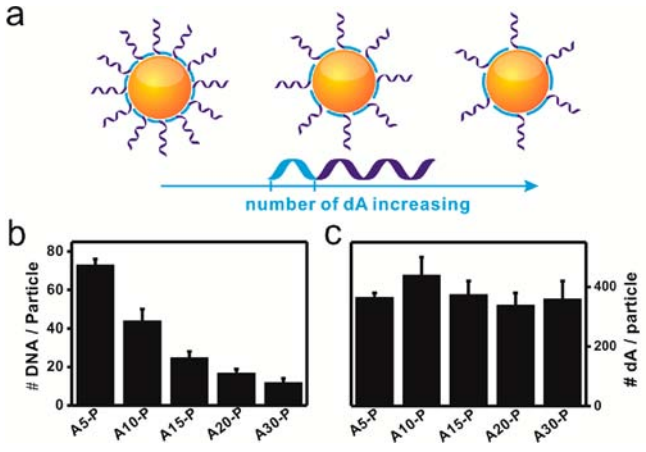

Figure 1. (a) Schematic for spatial control on AuNPs by varying the length of polyA blocks. (b) Surface densities of assembled diblock oligonucleotides (strand/AuNP). (c) Normalized densities in terms of adenine bases (base/AuNP).

oligonucleotides by using a displacement-based fluorescence method.[15] Indeed, the surface density decreased along with the length increase of the polyA block (Figure 1b), suggesting the increase of interstrand spacing on AuNPs. Interestingly, the decrease ratio in density almost coincides with the increase ratio in the length of polyA. Also interestingly, when the density was normalized in terms of A bases, nearly the same amount was obtained for all diblock oligonucleotides. This nice coincidence suggests that all A bases in the polyA block, independent of the length, are completely adsorbed on AuNPs to enable full surface coverage.

With the ability to spatially control the assembled oligonucleotides, we further investigate the hybridization ability of the recognition block on AuNPs. We prepared a series of nanoconjugates with various lengths of polyA blocks and tested their hybridization efficiency.[15] We found that the hybridization ability was remarkably improved as compared to the classic, thiolated oligonucleotide-based nanoconjugates (~5–10% as measured according to the previously reported protocol)[15] by an order of magnitude. More interesting, the hybridization efficiency was systematic enhanced with the increase of the polyA block length, with the $polyA_5$ being ~42% and $polyA_{30}$ reaching ~90% (Table S2, SI).

Such greatly improved hybridization efficiency at the polyA-coated AuNPs surface suggests that the recognition block is spatially controlled and adopts conformations that favors hybridization with complementary strands in solution.[16] Dynamic light scattering (DLS) analysis provides strong evidence (Figure S4, SI). AuNPs with polyA blocks (A5, A10, A15, A20, A30) exhibited uniform mean hydrodynamic diameters of 29–32 nm that are independent of the length of polyA. Hence the length of polyA only influences the surface density rather than the height of the adsorbed layer. As a comparison, the mean hydrodynamic diameter of thiol-DNA-coated AuNPs was only 21.6 nm. The difference (~10 nm) in hydrodynamic diameters between thiol and polyA-modified AuNPs suggests that the recognition block adopts a more extended and upright conformation than the oligonucleotide on the thiol-DNA-modified AuNPs. The finding that nearly all strands at the surface of polyA30-coated AuNPs are hybridizable is also consistent with the fact that increased interstrand spacing favors hybridization.[16a,17]

We next employed such nanoconjugates to construct a plasmonic DNA sensor. This design involves two types of DNA-AuNP nanoconjugates, each containing a unique oligonucleotide sequence that is complementary to part of the target sequence and flanks the target strand. The presence of the correct sequence of the target DNA aggregates the two types of nanoconjugates, resulting in a red-to-blue color change due to the shift of the plasmonic resonance peak of AuNPs.[7] When two types of diblock-based nanoconjugates ($polyA_{10}$-*b*-P1 and $polyA_{10}$-*b*-P2, Table S1, SI) were employed, we found that the target DNA (T1, Table S1, SI) nearly instantly induced the red-to-blue color change and the shift of the plasmonic resonance peak of AuNPs from 520 to 610 nm (Figure 2a). No color change was observed in the absence of target DNA, implying that this plasmonic sensor is highly specific.

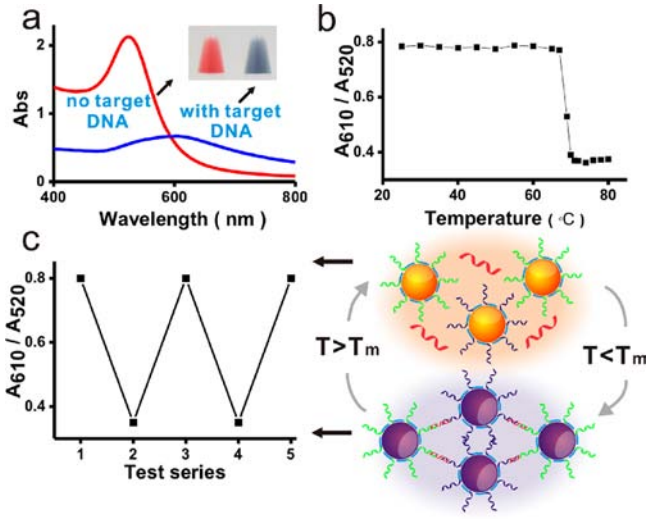

Figure 2. (a) UV–vis spectra and photographic images (inset) for diblock oligonucleotide–AuNP nanoconjugates in the absence and presence of target DNA. (b) Melt profile for nanoconjugates with the complementary sequence. (c) Sequential temperature cycles between 80 and 60 °C for nanoconjugates, absorption ratio (610 nm/520 nm, left panel), and schematic showing (right panel).

dx.doi.org/10.1021/ja304118z | J. Am. Chem. Soc. 2012, 134, 11876–11879

DNA–AuNP nanoconjugates are well-known to possess sharp melting transition, a collective property related to the high DNA density of AuNP.[7b] The diblock-AuNPs showed similar sharp transition in the melt profile (Figure 2b), with a similar transition point at ~70 °C, suggesting that the recognition block holds the similar thermodynamic property to those in the thiol-DNA-based nanoconjugates (Figure S5, SI). In addition, this melting process is completely reversible between the states of dispersion (red color) and aggregation (blue color) (Figure 2c).

We further explored the hybridization kinetics of nanoconjugates. The "sandwich" detection system involving three bodies (two types of thiol-DNA nanoconjugates and the target) is known to be notoriously slow in kinetics (nearly no color change until 12 h later)[7b] at room temperature and in the absence of proper accelerators[18] (Of note: the two-body system involving only two types of complementary thiol-DNA nanoconjugates is much faster in kinetics.) Interestingly, the diblock oligonucleotide-based nanoconjugates showed very fast hybridization kinetics. Color change was visualized nearly instantly upon mixing, and then blue color was observed in ~5 min. In the UV–vis absorption curves (Figure S6, SI), the plasmonic resonance peak of AuNPs was shifted by 80 nm in 40 min for the diblock system, while only by 13 nm for thiol-DNA.

Further quantitative analysis for this kinetic study was performed by curving fitting using the Avrami law.[18b,19] By regarding the hybridization-induced aggregation process of AuNPs as a nucleation and growth process, the absorption profiles could be fitted with eq 1:

$$\mathrm{Abs} = \mathrm{Abs}_0 \exp(-((t - t_0)/\tau)^n) \quad (1)$$

Here, t is the hybridization time, t_0 is reaction onset time, τ is the characteristic time that depends on reaction rate and aggregation geometry, and n is the Avrami exponent that is related to the physical mechanism of aggregate growth. The two parameters (τ and n) were determined to be 112 min and 0.77 (diblock) and 595 min and 0.99 (thiol-DNA), respectively (Figure 3a). Again, the smaller τ value of the former suggests faster kinetics, which is associated with the favorable conformation of the surface-tethered diblock oligonucleotides and the large lateral spacing between strands.

The fast kinetic of the nanoconjugates provides a new route to rapid bioassays. As a proof of concept, colorimetric DNA detection with the plasmonic AuNPs was tested using the nanoconjugates. This plasmonic DNA sensor exhibited visualizable color change within only 10 min (Figure 3b). By plotting the extinction ratio of 610 nm/520 nm to the target DNA concentration, we obtained a linear dose–response curve with a detection limit of 0.5 nM. In contrast, there was nearly no color change for thiol-DNA-based nanconjugates even with 10 nM target DNA.

AuNPs have shown great promise as the building block for a wide range of applications including high-sensitivity diagnostics,[6c] nanocarriers for intracelluar delivery,[6b] and bottom-up construction of crystalline[20] or plasmonic nanostructures.[6d] Many of these applications take the advantage of the collective property of the nanoconjugate system that accommodates tens to hundreds of oligonucleotides on a single nanoparticle. Nevertheless, the high density of oligonucleotides at the AuNP surface also impedes their hybridization with the target DNA strands,[21] which is another critical factor for some applications (e.g., sensitivity of AuNPs-based sensors). This apparent

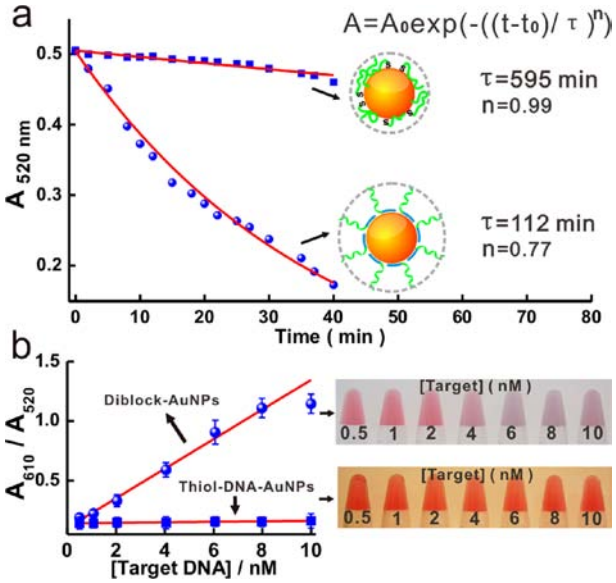

Figure 3. (a) The kinetic plots for nanoconjugates hybridized with the target DNA, as monitored by absorption at 520 nm, and fitted with the Avrami law's eqation (red line). (b) Dose–response curves and photographic images for DNA detection by using two types of nanoconjugates (in 10 min).

dilemma can be readily circumvented with our new strategy, as evidenced by precise spatial control and high hybridization ability of the diblock oligonucleotide-based AuNP nanoconjugates. Also, this strategy is much more convenient and controllable than the previously reported method with displacement reagent 6-mercapto-1-heanol (MCH), which is likely to result in contamination and uncertainty in displacement.[22] Given the great enhancement in the hybridization ability, we expect that ultrahigh sensitivity for DNA detection might be realized when this new type of nanoconjugates is coupled with instrumental analysis (e.g., Raman or electronic).[23]

The introduction of diblock oligonucleotides the in AuNPs-based system offers several combined advantages. First, unlike thiolated oligonucleotides, diblock oligonucleotides are natural sequences that are essentially free of any modification, hence the synthesis cost is reduced and possible contamination is prevented. Second, since polyA not only offers the anchoring function but also effectively blocks nonspecific DNA–Au binding, our new strategy provides a reproducible means to prepare nanoconjugates with well-defined surface density and favorable hybridization ability. Finally, given the high and tunable hybridization ability of diblock oligonucleotide system in both thermodynamics and kinetics, it is envisioned that such nanoconjugates are well suited to bottom-up construct complex nanostructures and nanodevice.

■ ASSOCIATED CONTENT

Ⓢ Supporting Information

Experimental procedures and additional tables and figures. This material is available free of charge via the Internet at http://pubs.acs.org.

■ AUTHOR INFORMATION

Corresponding Author

fchh@sinap.ac.cn; liuhuajie@sinap.ac.cn

Author Contributions

[§]These authors contributed equally.

Notes

The authors declare no competing financial interest.

■ ACKNOWLEDGMENTS

This work was supported by the National Basic Research Program (973 Program 2012CB932600), NSFC (21075128, 20902096, 21073221, 21103219, 90913014), Shanghai Pujiang Program (11PJ1412000), and Chinese Academy of Sciences.

■ REFERENCES

(1) (a) Seeman, N. C. *Nature* **2003**, *421*, 427. (b) Pinheiro, A. V.; Han, D. R.; Shih, W. M.; Yan, H. *Nat. Nanotechnol.* **2011**, *6*, 763.
(2) Gothelf, K. V.; LaBean, T. H. *Org. Biomol. Chem.* **2005**, *3*, 4023.
(3) Liu, D.; Cheng, E.; Yang, Z. *NPG Asia Mater.* **2011**, *3*, 109.
(4) Aldaye, F. A.; Palmer, A. L.; Sleiman, H. F. *Science* **2008**, *321*, 1795.
(5) (a) Zhang, T.; Yang, Z.; Liu, D. *Nanoscale* **2011**, *3*, 4015. (b) Zhang, T.; Chen, P.; Sun, Y.; Xing, Y.; Yang, Y.; Dong, Y.; Xu, L.; Yang, Z.; Liu, D. *Chem. Commun.* **2011**, *47*, 5774. (c) Li, Z.; Cheng, E.; Huang, W.; Zhang, T.; Yang, Z.; Liu, D.; Tang, Z. *J. Am. Chem. Soc.* **2011**, *133*, 15284. (d) Zhang, T.; Dong, Y.; Sun, Y.; Chen, P.; Yang, Y.; Zhou, C.; Xu, L.; Yang, Z.; Liu, D. *Langmuir* **2012**, *28*, 1966.
(6) (a) Katz, E.; Willner, I. *Angew. Chem., Int. Ed.* **2004**, *43*, 6042. (b) Rosi, N. L.; Giljohann, D. A.; Thaxton, C. S.; Lytton-Jean, A. K. R.; Han, M. S.; Mirkin, C. A. *Science* **2006**, *312*, 1027. (c) Rosi, N. L.; Mirkin, C. A. *Chem. Rev.* **2005**, *105*, 1547. (d) Tan, S. J.; Campolongo, M. J.; Luo, D.; Cheng, W. *Nat. Nanotechnol.* **2011**, *6*, 268. (e) Cheng, W. L.; Park, N. Y.; Walter, M. T.; Hartman, M. R.; Luo, D. *Nat. Nanotechnol.* **2008**, *3*, 682. (f) Cheng, W. L.; Campolongo, M. J.; Cha, J. J.; Tan, S. J.; Umbach, C. C.; Muller, D. A.; Luo, D. *Nat. Mater.* **2009**, *8*, 519.
(7) (a) Mirkin, C. A.; Letsinger, R. L.; Mucic, R. C.; Storhoff, J. J. *Nature* **1996**, *382*, 607. (b) Elghanian, R.; Storhoff, J. J.; Mucic, R. C.; Letsinger, R. L.; Mirkin, C. A. *Science* **1997**, *277*, 1078.
(8) Parak, W. J.; Pellegrino, T.; Micheel, C. M.; Gerion, D.; Williams, S. C.; Alivisatos, A. P. *Nano Lett.* **2003**, *3*, 33.
(9) Tang, J.; Huo, Z.; Brittman, S.; Gao, H.; Yang, P. *Nat. Nanotechnol.* **2011**, *6*, 568.
(10) Kim, H.-C.; Park, S.-M.; Hinsberg, W. D. *Chem. Rev.* **2011**, *110*, 146.
(11) (a) Keefe, A. D.; Pai, S.; Ellington, A. *Nat. Rev. Drug Discovery* **2010**, *9*, 537. (b) Liu, H.; Liu, D. *Chem. Commun.* **2009**, 2625. (c) Liu, J. W.; Cao, Z. H.; Lu, Y. *Chem. Rev.* **2009**, *109*, 1948. (d) Willner, I.; Shlyahovsky, B.; Zayats, M.; Willner, B. *Chem. Soc. Rev.* **2008**, *37*, 1153.
(12) (a) Kwak, M.; Herrmann, A. *Angew. Chem., Int. Ed.* **2010**, *49*, 8574. (b) Kwak, M.; Herrmann, A. *Chem. Soc. Rev.* **2011**, *20*, 5745.
(13) Tikhomirov, G.; Hoogland, S.; Lee, P. E.; Fischer, A.; Sargent, E. H.; Kelley, S. O. *Nat. Nanotechnol.* **2011**, *6*, 485.
(14) (a) Opdahl, A.; Petrovykh, D. Y.; Kimura-Suda, H.; Tarlov, M. J.; Whitman, L. J. *Proc. Natl. Acad. Sci. U.S.A.* **2007**, *104*, 9. (b) Schreiner, S. M.; Shudy, D. F.; Hatch, A. L.; Opdahl, A.; Whitman, L. J.; Petrovykh, D. Y. *Anal. Chem.* **2010**, *82*, 2803.
(15) Demers, L. M.; Mirkin, C. A.; Mucic, R. C.; Reynolds, R. A., III; Letsinger, R. L.; Elghanian, R.; Viswanadham, G. *Anal. Chem.* **2000**, *72*, 5535.
(16) (a) Gong, P.; Levicky, R. *Proc. Natl. Acad. Sci. U.S.A.* **2008**, *105*, 5301. (b) Levicky, R.; Horgan, A. *Trends Biotechnol.* **2005**, *23*, 143.
(17) (a) Pei, H.; Lu, N.; Wen, Y. L.; Song, S. P.; Liu, Y.; Yan, H.; Fan, C. H. *Adv. Mater.* **2010**, *22*, 4754. (b) Pei, H.; Wan, Y.; Li, J.; Hu, H. Y.; Su, Y.; Huang, Q.; Fan, C. H. *Chem. Commun.* **2011**, *47*, 6254.
(18) (a) Prigodich, A. E.; Lee, O.-S.; Daniel, W. L.; Seferos, D. S.; Schatz, G. C.; Mirkin, C. A. *J. Am. Chem. Soc.* **2010**, *132*, 10638. (b) Maye, M. M.; Nykypanchuk, D.; Van der Lelie, D.; Gang, O. *J. Am. Chem. Soc.* **2006**, *128*, 14020.
(19) (a) Rikvold, P. A.; Tomita, H.; Miyashita, S.; Sides, S. W. *Phys. Rev. E* **1994**, *49*, 5080. (b) Avrami, M. J. *Chem. Phys.* **1940**, *8*, 212.
(20) (a) Nykypanchuk, D.; Maye, M. M.; van der Lelie, D.; Gang, O. *Nature* **2008**, *451*, 549. (b) Park, S. Y.; Lytton-Jean, A. K. R.; Lee, B.; Weigand, S.; Schatz, G. C.; Mirkin, C. A. *Nature* **2008**, *451*, 553.
(21) Pena, S. R. N.; Raina, S.; Goodrich, G. P.; Fedoroff, N. V.; Keating, C. D. *J. Am. Chem. Soc.* **2002**, *124*, 7314.
(22) Park, S.; Brown, K. A.; Hamad-Schifferli, K. *Nano Lett.* **2004**, *4*, 1925.
(23) (a) Cao, Y. W. C.; Jin, R. C.; Mirkin, C. A. *Science* **2002**, *297*, 1536. (b) Zhang, J.; Song, S. P.; Zhang, L. Y.; Wang, L. H.; Wu, H. P.; Pan, D.; Fan, C. H. *J. Am. Chem. Soc.* **2006**, *128*, 8575. (c) Zhang, J.; Song, S. P.; Wang, L. H.; Pan, D.; Fan, C. H. *Nat. Protoc.* **2007**, *2*, 2888. (d) Xue, X.; Xu, W.; Wang, F.; Liu, X. *J. Am. Chem. Soc.* **2009**, *131*, 11668.